VIP *The following Communications have been judged by at least two referees to be "very important papers" and will be published online at www.angewandte.org soon:*

*S. Wittrock, T. Becker, H. Kunz**
Synthetic Vaccines from Tumor-Associated Glycopeptide Antigens by Immunocompatible Linking to Bovine Serum Albumin through Thioether Formation

M. Manoli, R. D. L. Johnstone, S. Parsons, M. Murrie, M. Affronte, M. Evangelisti, E. K. Brechin**
A Ferromagnetic Mixed-Valent Mn Supertetrahedron: Towards Low-Temperature Magnetic Refrigeration with Molecular Clusters

*J.-D. Ye, N.-S. Li, Q. Dai, J. A. Piccirilli**
The Mechanism of RNA Strand Scission: An Experimental Measure of β_{nuc}

X. Lou, G. Zhang, I. Herrera, R. Kinach, O. Ornatsky, V. Baranov, M. Nitz*, M. A. Winnik**
Polymer-Based Elemental Tags for Sensitive Bioassays

*Y. Sawada, K. Matsumoto, T. Katsuki**
Titanium-Catalyzed Asymmetric Epoxidation of Nonactivated Olefins with Hydrogen Peroxide

*L. Alaerts, C. E. A. Kirschhock, M. Maes, M. A. v. d. Veen, V. Finsy, A. Depla, J. A. Martens, G. V. Baron, P. A. Jacobs, J. F. M. Denayer, D. E. De Vos**
Selective Adsorption and Separation of Xylene Isomers and Ethylbenzene with the Microporous Vanadium(IV) Terephthalate MIL-47

News

Books

Highlights

Back to basics: Ligand design has allowed two longstanding limitations of Pd-catalyzed C–N and C–O coupling reactions to be overcome. The use of specific sterically demanding electron-rich phosphine ligands makes it possible for ammonia and potassium hydroxide to act as coupling partners in palladium-catalyzed coupling with aryl halides.

NH_3 and KOH Couplings

M. C. Willis* ____ **3402 – 3404**

Palladium-Catalyzed Coupling of Ammonia and Hydroxide with Aryl Halides: The Direct Synthesis of Primary Anilines and Phenols

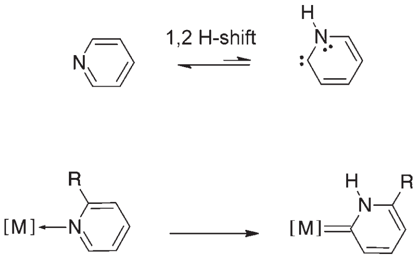

70 years ago the existence of the 2-carbene isomer of pyridine, which arises by pyridine–carbene tautomerization (see scheme), was postulated. Now it has been prepared from pyridine as a stable carbene complex by metal-induced C–H activation. This pyridine–carbene tautomerization is described and discussed along with other analogous carbene tautomerization reactions.

Pyridine–Carbene Tautomerization

D. Kunz* ____ **3405 – 3408**

Synthetic Routes to N-Heterocyclic Carbene Complexes: Pyridine–Carbene Tautomerizations

Contents

Reviews

Synthetic Methods

A. Fürstner,* P. W. Davies* _ **3410–3449**

Catalytic Carbophilic Activation: Catalysis by Platinum and Gold π Acids

The reactivity of π-acidic metal catalysts has been correlated to known structural data. Through this comparison, the apparently disparate electrophilic metal carbene and nonclassical carbocation explanations (see picture), used in the literature to rationalize the diverse range of transformations possible under platinum and gold catalysis, come together under a reactivity profile through which this field may be rationalized.

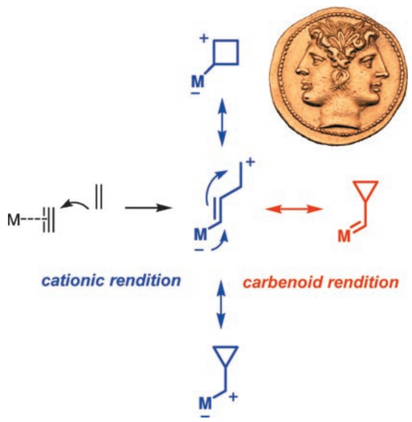

Communications

Energy-Transfer Systems

K. Becker, P. G. Lagoudakis, G. Gaefke, S. Höger,* J. M. Lupton* ___ **3450–3455**

Exciton Accumulation in π-Conjugated Wires Encapsulated by Light-Harvesting Macrocycles

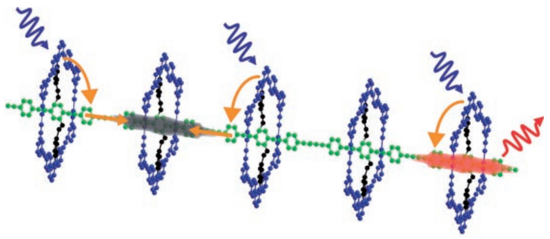

Insulated wires: Light harvesting was demonstrated from a macrocyclic "tube" to covalently bound π-conjugated polymers encapsulated within (see picture). The multichromophoric polymer core allows accumulation of excitation energy. The high intramolecular mobility of these excitations leads to a dependence of the emission dynamics on chain length.

Magnetic Porous Materials

X.-M. Zhang,* Z.-M. Hao, W.-X. Zhang, X.-M. Chen ___ **3456–3459**

Dehydration-Induced Conversion from a Single-Chain Magnet into a Metamagnet in a Homometallic Nanoporous Metal–Organic Framework

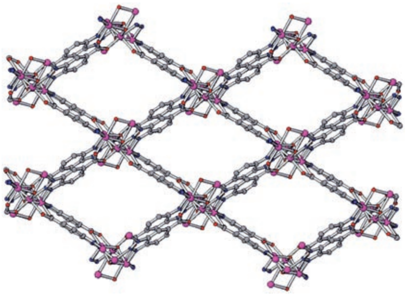

A change for the meta: On dehydration, a 3D homometallic porous organic–inorganic framework constructed from $\{Co_3(OH)_2\}$ chains (see structure, pink Co, red O, blue N, gray C) undergoes a transition from being a single-chain magnet into a metamagnet. Apart from the loss of solvent water molecules, the dehydration leaves the framework structure largely unchanged.

For the USA and Canada:
ANGEWANDTE CHEMIE International Edition (ISSN 1433-7851) is published weekly by Wiley-VCH, PO Box 191161, 69451 Weinheim, Germany. Air freight and mailing in the USA by Publications Expediting Inc., 200 Meacham Ave., Elmont, NY 11003. Periodicals postage paid at Jamaica, NY 11431. US POSTMASTER: send address changes to *Angewandte Chemie*, Wiley-VCH, 111 River Street, Hoboken, NJ 07030. Annual subscription price for institutions: US$ 5685/5168 (valid for print and electronic / print or electronic delivery); for individuals who are personal members of a national chemical society prices are available on request. Postage and handling charges included. All prices are subject to local VAT/sales tax.

Fluorescent Probes

H. M. Kim, C. Jung, B. R. Kim, S.-Y. Jung, J. H. Hong, Y.-G. Ko, K. J. Lee, B. R. Cho* ______ **3460 – 3463**

Environment-Sensitive Two-Photon Probe for Intracellular Free Magnesium Ions in Live Tissue

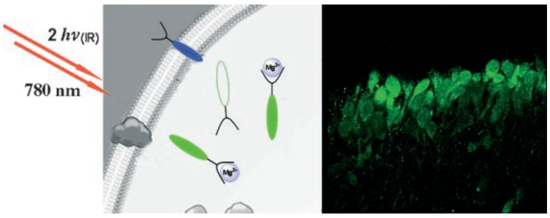

“Green” emission: A novel two-photon fluorescent probe that can detect intracellular free Mg^{2+} ions at a depth of a few hundred micrometers in live tissue was developed. The emission from the Mg^{2+}–probe complex (green) shows little interference from association of the probe with other intracellular metal ions or with the cell membrane (blue).

Nanostructures

G. Cui, L. Zhi,* A. Thomas, U. Kolb, I. Lieberwirth, K. Müllen* ___ **3464 – 3467**

One-Dimensional Porous Carbon/Platinum Composites for Nanoscale Electrodes

Current developments: The combination of a template method with electrochemical procedures has led to the controlled preparation of 1D nanoscale carbon/platinum electrodes with large surface areas and with small platinum nanoparticles homogeneously dispersed in the interconnected porous carbon matrix (see TEM images). The electrodes display excellent catalytic activities in the oxygen electroreduction.

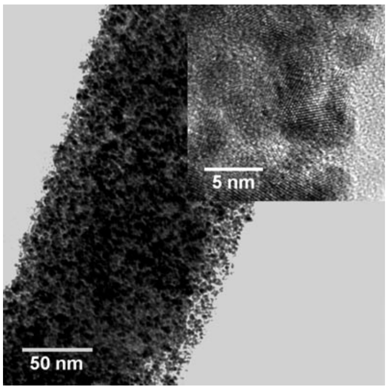

Colorimetric Screening

X. Xu, M. S. Han, C. A. Mirkin* ______ **3468 – 3470**

A Gold-Nanoparticle-Based Real-Time Colorimetric Screening Method for Endonuclease Activity and Inhibition

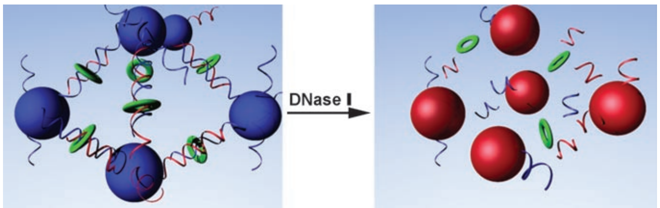

On the small screen: Aggregates of gold nanoparticles interconnected by DNA duplexes (see scheme, left) are bluish-purple. Cleavage of the duplexes by deoxyribonuclease I (DNase I) releases the nanoparticles (right), producing a bluish-purple-to-red color change. This color change can be used to monitor the activity (and inhibition) of the enzyme.

Polymer Nanocapsules

D. Kim, E. Kim, J. Kim, K. M. Park, K. Baek, M. Jung, Y. H. Ko, W. Sung, H. S. Kim, J. H. Suh, C. G. Park, O. S. Na, D.-k. Lee, K. E. Lee, S. S. Han, K. Kim* **3471 – 3474**

Direct Synthesis of Polymer Nanocapsules with a Noncovalently Tailorable Surface

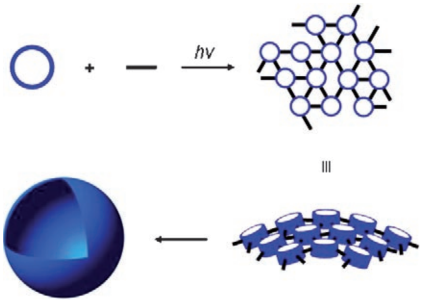

Hollow out your pumpkin: The direct synthesis of approximately 100-nm-diameter polymer nanocapsules was carried out in the absence of preorganized structures or templates. The method appears to be applicable to any monomer that has a flat core and multiple polymerizable groups at the periphery (see picture). The surface properties of the polymer shell, which comprises cucurbituril, can be easily tailored through host–guest chemistry.

Angewandte Chemie
CHEMISTRY A EUROPEAN JOURNAL
CHEMISTRY AN ASIAN JOURNAL
EurJIC
EurJOC
CHEMIE IN UNSERER ZEIT
CHEMBIOCHEM
CHEMMEDCHEM
CHEMPHYSCHEM
Advanced Synthesis & Catalysis
ZAAC

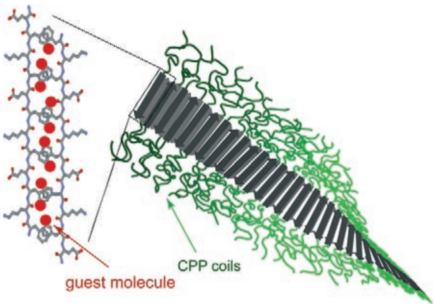

Wrap it up: Nanoribbons coated with cell-penetrating peptides (CPPs) allowed the encapsulation of hydrophobic guest molecules. The nanoassembly internalized into mammalian cells with high efficiency and showed selective intracellular compartmentalization owing to its sensitivity to the solution environment.

Cell-Penetrating Peptides

Y.-b. Lim, E. Lee, M. Lee* — **3475 – 3478**

Cell-Penetrating-Peptide-Coated Nanoribbons for Intracellular Nanocarriers

---

One for the road: The potential-energy hyperface along the pathway of the formation of an abasic site (P_{abasic}) suggests that low-energy electrons (LEEs) might induce the formation of such a site at the 3′ end of a DNA double helix with the strand ended in a cytidine residue. Attachment of these LEEs to a DNA helix might significantly contribute to radiation-induced DNA damage. TS = transition state.

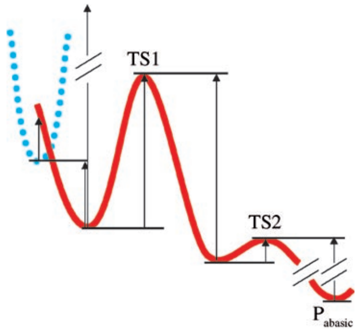

DNA Abasic Sites

J. Gu,* J. Wang, J. Rak, J. Leszczynski* ———— **3479 – 3481**

Findings on the Electron-Attachment-Induced Abasic Site in a DNA Double Helix

---

No empty FRET: The microfluidic control of fluorescence resonance energy transfer (FRET) has been demonstrated, and the FRET limit has been broken with a quantum-dot (QD)-based DNA nanosensor in a microfluidic flow. This nanosensor can detect long nucleic acids that have separation distances far beyond the range of FRET and whose detection is not feasible with conventional FRET-based assays.

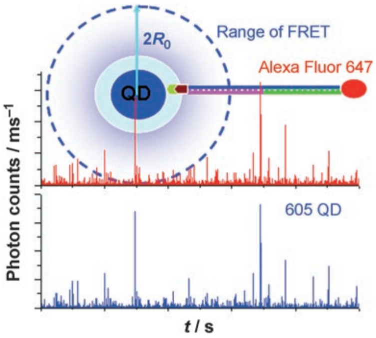

DNA Sensors

C. Y. Zhang, L. W. Johnson* **3482 – 3485**

Microfluidic Control of Fluorescence Resonance Energy Transfer: Breaking the FRET Limit

---

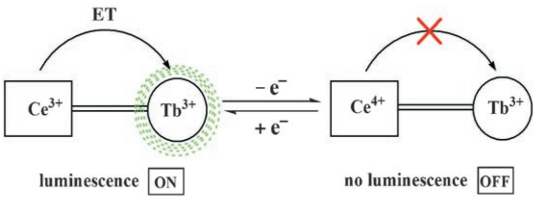

On and off and on again: High-quality $CePO_4$:Tb^{3+} nanowires were prepared easily in high yields at room temperature. The resulting 1D nanostructures exhibit Ce^{3+}-sensitized terbium(III) luminescence (green). Oxidation of Ce^{3+} results in an absence of energy transfer (ET) from Ce^{4+} to Tb^{3+} and thus no green emission of the sample (see picture). The effect can be reversed by reduction, thus giving a reversible luminescent switch.

Functional Nanomaterials

Q. Li, V. W.-W. Yam* ——— **3486 – 3489**

Redox Luminescence Switch Based on Energy Transfer in $CePO_4$:Tb^{3+} Nanowires

Polyoxometalate Anions

S. Wang,* X. Lin, Y. Wan, W. Yang,
S. Zhang, C. Lu, H. Zhuang **3490 – 3493**

A Large, Bowl-Shaped $\{Mo_{51}V_9\}$ Polyoxometalate

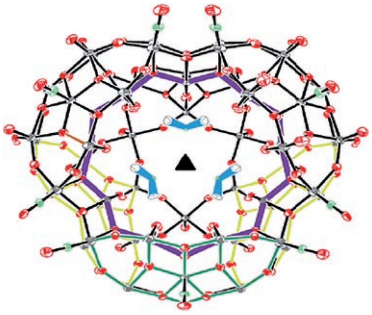

Bowled over: A bowl-shaped $\{Mo_{51}V_9\}$ polyoxometalate anion (see picture) is produced in a hydrothermal synthesis by a redox self-assembly process. This new compound has different building blocks and linkages to previously reported polyoxometalates (see structure; N green, O red, Mo/V gray, threefold axis indicated by black triangle).

Ligand Substitution

E. J. Welch, J. R. Long* ——— **3494 – 3496**

Synthesis and Ligand-Exchange Kinetics of the Solvated Trigonal-Prismatic Clusters $[W_6CCl_{12}L_6]^{2+}$ (L = dmf, py)

Trading places: The first terminal-ligand substitution reactions on the trigonal-prismatic cluster $[W_6CCl_{18}]^{2-}$ are reported. The new cluster $[W_6CCl_{12}(SO_3CF_3)_6]^{2-}$ is a convenient precursor for solvated $[W_6CCl_{12}]^{2+}$ cluster cores. Self-exchange kinetics experiments on a pyridine-substituted variant (see picture; black W, green Cl, blue N, dark gray C) reveal that the core is classified as inert.

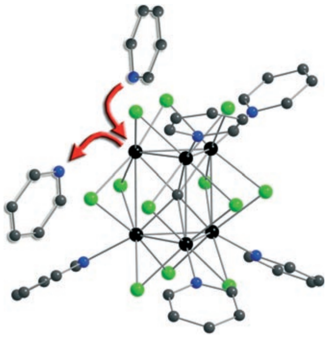

Organic Ferroelectrics

S. Horiuchi,* R. Kumai,
Y. Tokura ——— **3497 – 3501**

A Supramolecular Ferroelectric Realized by Collective Proton Transfer

Cooperative crystals: In ferroelectric cocrystals of iodanilic acid (see picture, orange) and 5,5′-dimethyl-2,2′-bipyridine (green), the molecules are linked into polar chains by O–H···N and N⁺–H···O⁻ hydrogen bonds. The application of a small electric field (*E*) effects a cooperative proton transfer across the hydrogen bonds, which is accompanied by a reversal of the polarity (*P*).

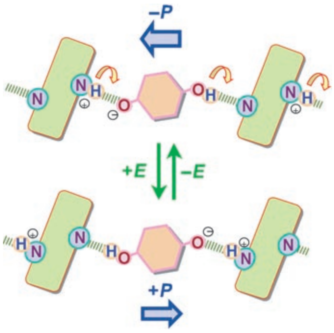

RNA Modifications

D. A. Baum,
S. K. Silverman* ——— **3502 – 3504**

Deoxyribozyme-Catalyzed Labeling of RNA

Tag team: A deoxyribozyme is used in a general strategy for site-specific covalent modification of RNA. This strategy was used to append the fluorescence resonant energy transfer (FRET) pair, fluorescein and tetramethylrhodamine (tamra), to the 160-nucleotide P4–P6 RNA, thereby enabling a FRET experiment to be performed for this RNA.

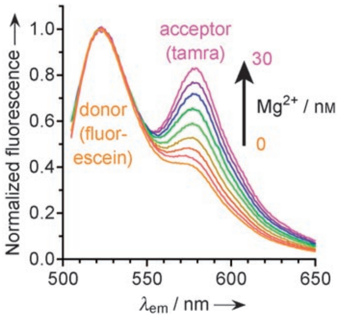

Singled out: Specific high-affinity binding to and activation of nicotinic acetylcholine receptors (nAChRs) by fluorescent epibatidine (EPB) agonists is detected by fluorescence microscopy and electrophysiology (see picture). The optical and pharmacological properties of these compounds allow single-channel/single-molecule experiments at the surface of living cells, and investigation of channel gating and receptor trafficking.

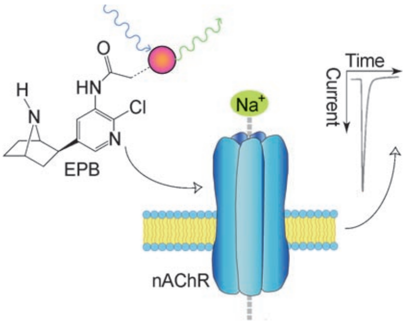

Receptor Agonists

J. Grandl, E. Sakr, F. Kotzyba-Hibert,
F. Krieger, S. Bertrand, D. Bertrand,
H. Vogel,* M. Goeldner,*
R. Hovius ________ 3505 – 3508

Fluorescent Epibatidine Agonists for Neuronal and Muscle-Type Nicotinic Acetylcholine Receptors

---

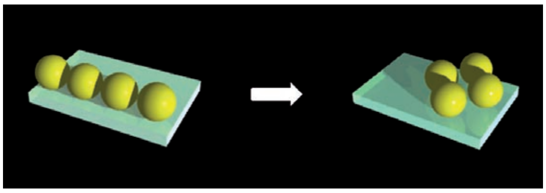

Changing places: A chain-to-sheet rearrangement of the Pd_4 moiety (see picture; spheres: Pd, support: organic ligand) takes place during the exchange of one perylene or fluoranthene ligand of a bis(perylene) or a bis(fluoranthene) tetrapalladium sandwich complex by 1,3,5,7-cyclooctatetraene. These findings are established by X-ray crystallography and NMR spectroscopy.

Multinuclear Sandwich Complexes

T. Murahashi,* N. Kato, T. Uemura,
H. Kurosawa ________ 3509 – 3512

Rearrangement of a Pd_4 Skeleton from a 1D Chain to a 2D Sheet on the Face of a Perylene or Fluoranthene Ligand Caused by Exchange of the Binder Molecule

---

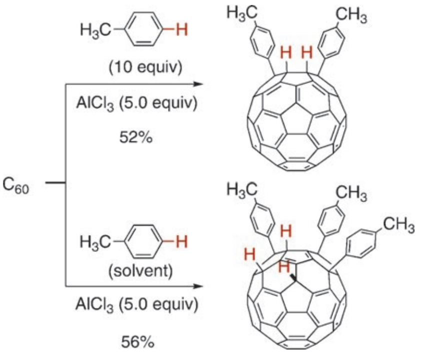

Functionalization of fullerenes can be achieved inexpensively by Friedel–Crafts reaction. For instance, treatment of [60]fullerene with $AlCl_3$ in toluene gave mono-, di-, and tritolyltrihydro[60]fullerenes in moderate to good yields (see scheme). The structures of the products were determined by crystallography and derivatization.

Fullerene Chemistry

A. Iwashita, Y. Matsuo,*
E. Nakamura* ________ 3513 – 3516

$AlCl_3$-Mediated Mono-, Di-, and Trihydroarylation of [60]Fullerene

---

Telling FIBs: Identification of the exact size and shape of a nanoparticle is crucial for direct comparison of experimental results with theoretical predictions. A focused ion beam (FIB) registration method enables routine spectroscopic and high-resolution microscopic experiments to be carried out on the same nanoparticle (see picture).

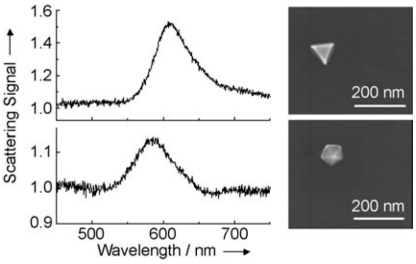

Single-Particle Spectroscopy

C. Novo, A. M. Funston,
I. Pastoriza-Santos, L. M. Liz-Marzán,
P. Mulvaney* ________ 3517 – 3520

Spectroscopy and High-Resolution Microscopy of Single Nanocrystals by a Focused Ion Beam Registration Method

Contents

Electron Transfer

A. Mateo-Alonso,* C. Ehli,
G. M. A. Rahman, D. M. Guldi,*
G. Fioravanti, M. Marcaccio, F. Paolucci,*
M. Prato* ______________ **3521 – 3525**

Tuning Electron Transfer through Translational Motion in Molecular Shuttles

Shuttling rules! A bistable fullerene-stoppered molecular shuttle equipped with two ferrocene electron donors on the macrocycle has been prepared. A controlled positional change of the ferrocene groups along the thread results in different spatial arrangements of the electroactive units and allows the kinetics of the electron transfer and the lifetime of the charged-separated state to be modulated/fine-tuned (see picture).

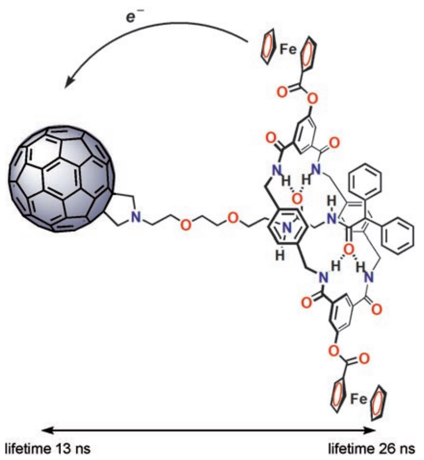

Total Synthesis

M. Sani, G. Fossati, F. Huguenot,
M. Zanda* ______________ **3526 – 3529**

Total Synthesis of Tubulysins U and V

Meeting the challenge: A reliable and modular reaction sequence has been developed for the synthesis of the challenging tubulysin framework. This route allows preparation of hundreds of milligrams of the stereochemically pure tetrapeptides (see picture), which are produced in small amounts by two different species of myxobacteria. Thus, full biological evaluation of the tubulysins and their analogues is now a real possibility.

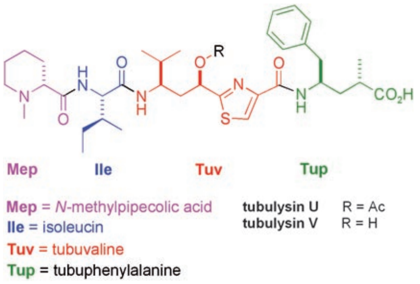

Electrocatalysis

B. E. Hayden,* D. Pletcher,
J.-P. Suchsland ______________ **3530 – 3532**

Enhanced Activity for Electrocatalytic Oxidation of Carbon Monoxide on Titania-Supported Gold Nanoparticles

Support makes the difference: Investigation of particle-size- and substrate-dependent activity for the electrochemical oxidation of CO provides an opportunity to consider the origin of the unique activity of supported Au nanoparticles in a new light. Furthermore, manipulation of catalytic activity by particle size and support provides an important tool for the future optimization of electrocatalysts.

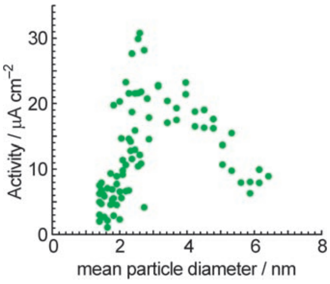

Metal–Metal Interactions

M.-M. Rohmer,* I. P.-C. Liu, J.-C. Lin,
M.-J. Chiu, C.-H. Lee, G.-H. Lee,
M. Bénard, X. López,
S.-M. Peng* ______________ **3533 – 3536**

Structural, Magnetic, and Theoretical Characterization of a Heterometallic Polypyridylamide Complex

A heterometallic backbone has been obtained for the first time in a trinuclear complex of bis(2-pyridyl)amide (dpa), namely, $[Co_2PdCl_2(dpa)_4]$ (**1**). The crystal structure (depicted), magnetic measurements, and DFT calculations suggest that its ground state results from coupling of two high-spin Co^{II} ions separated by a magnetically inactive Pd center. Hence, the magnetic behavior of Co^{II} in **1** strongly differs from that in its tricobalt homologue.

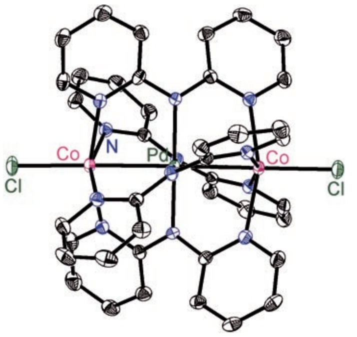

On the fast track: A molecular shuttle has been synthesized, whose ring incorporates an 8,8′-diphenyl-3,3′-biisoquinoline chelating unit. This unit is both endocyclic and not sterically hindering (see picture), which leads to remarkably fast shuttling motions (milliseconds) of the copper-complexed ring between two stations.

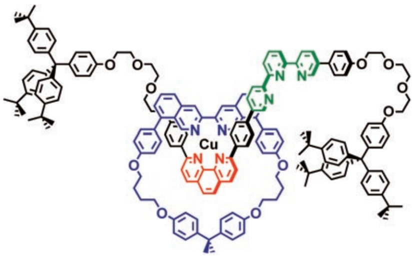

Molecular Devices

F. Durola, J.-P. Sauvage* ___ **3537 – 3540**

Fast Electrochemically Induced Translation of the Ring in a Copper-Complexed [2]Rotaxane: The Biisoquinoline Effect

---

Coming full circle: Bis(alkenyl)-platinum(II) complexes cis-[$L_2Pt\{(CH_2)_nCH{=}CH_2\}_2$] ($L = PPh_3$ or $L_2 = Ph_2P(CH_2)_3PPh_2$; $n = 3–6$) have been prepared and fully characterized. Ring-closing metathesis leads to new platinacycloalkenes, which can be hydrogenated to platinacycloalkanes with 9-, 11-, 13-, and 15-membered rings (see picture for 15-membered ring; Pt green, P orange, C blue, H white).

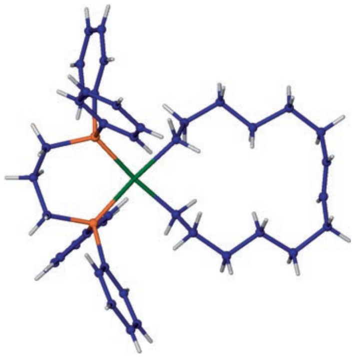

Platinum Metallacycles

A. Sivaramakrishna, H. Su, J. R. Moss* ___ **3541 – 3543**

High-Yield Synthesis of Medium and Large Platinacycloalkanes from Bis(alkenyl) Precursors

---

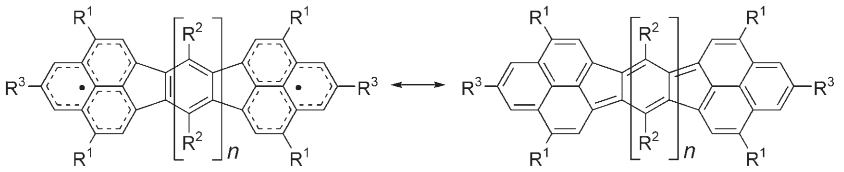

1b ($n = 1$, $R^2 = Ph$, R^1, $R^3 = H$) : $\sigma^{(2)}$ **= 424 GM (1425 nm), 5450 GM (880 nm)**
2 ($n = 2$, $R^1 = H$, $R^2 = Ph$, $R^3 = t$Bu) : $\sigma^{(2)}$ **= 890 GM (1500 nm), 8300 GM (1055 nm)**

Ones and twos: The two-photon absorption cross sections ($\sigma^{(2)}$) of singlet diradical hydrocarbons with phenalenyl peripheral groups (see scheme) are larger than those of closed-shell aromatic hydrocarbons by an order of magnitude or more and are comparable to those of π-conjugated compounds with strong electron donor or acceptor substituents. A significant increase in cross section was also observed in the resonance-enhanced region.

Radicals

K. Kamada,* K. Ohta, T. Kubo, A. Shimizu, Y. Morita, K. Nakasuji, R. Kishi, S. Ohta, S. Furukawa, H. Takahashi, M. Nakano ___ **3544 – 3546**

Strong Two-Photon Absorption of Singlet Diradical Hydrocarbons

---

Simple synthesis of a potent probe: An efficient solid-phase synthesis of Glu^7-phalloidin (the resin-bound cyclic peptide shown) features the one-pot I_2-mediated deprotection of S-tritylcysteine and formation of the Cys–Trp thioether bridge. A fluorescent conjugate of the resulting phalloidin analogue shows specific staining of F-actin (filamentous actin) in fixed mammalian epithelial cells (see fluorescence micrograph). Fmoc = 9-fluorenylmethoxycarbonyl.

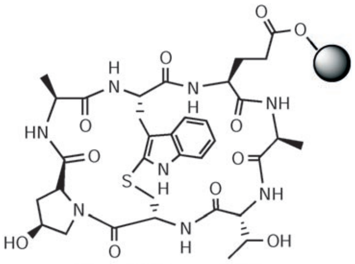

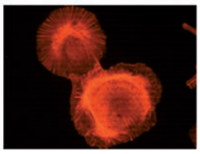

Cyclic Peptides

L. A. Schuresko, R. S. Lokey* ___ **3547 – 3549**

A Practical Solid-Phase Synthesis of Glu^7-Phalloidin and Entry into Fluorescent F-Actin-Binding Reagents

Electrolytic Fluorination

T. Tajima,* A. Nakajima, Y. Doi,
T. Fuchigami ______ **3550–3552**

Anodic Fluorination Based on Cation Exchange between Alkali-Metal Fluorides and Solid-Supported Acids

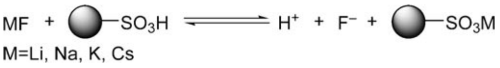

Positively shocking: The interchange of cations between alkali-metal fluorides and solid-supported acids (see picture) in an electrolytic system promotes the anodic fluorination of organic compounds to give the corresponding fluorinated products in good to excellent yields.

Hydrogen-Bonded Complex

J. Yuasa, S. Yamada,
S. Fukuzumi* ______ **3553–3555**

Direct EPR Detection of a Hydrogen-Bonded Complex between a Semiquinone Radical Anion and a Protonated Amino Acid, and Electron Transfer Driven by Hydrogen Bonding

Strong hydrogen bonding in a complex of a semiquinone radical anion and protonated histidine (His·2 H$^+$), detected for the first time by EPR spectroscopy during photoinduced electron transfer from 10,10′-dimethyl-9,9′-biacridine (D) to 1-(*p*-tolylsulfinyl)-2,5-benzoquinone in the presence of His·2 H$^+$ (picture, top), was revealed by the presence in the EPR spectrum (picture, bottom) of superhyperfine splitting caused by the NH$_3^+$ group.

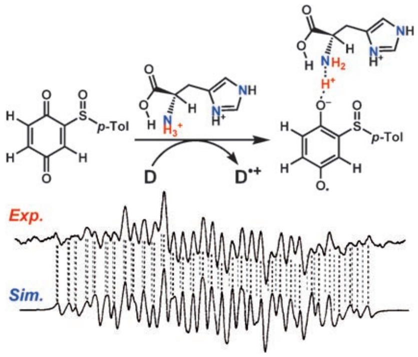

Homogeneous Catalysis

N. A. Strotman, S. Sommer,
G. C. Fu* ______ **3556–3558**

Hiyama Reactions of Activated and Unactivated Secondary Alkyl Halides Catalyzed by a Nickel/Norephedrine Complex

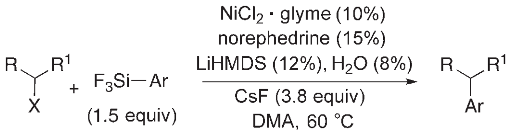

An active partner: Nickel in combination with an amino alcohol ligand (norephedrine) was found to provide the most versatile and efficient catalyst for Hiyama cross-coupling reactions of alkyl electrophiles that has been described to date. Unprecedented Hiyama reactions of activated secondary alkyl bromides were achieved, as were the first Hiyama couplings of (activated) alkyl chlorides (see scheme, X = Br, Cl; HMDS = 1,1,1,3,3,3-hexamethyldisilazane, DMA = *N*,*N*-dimethylacetamide).

Biomaterials

J. H. Exler, D. Hümmerich,
T. Scheibel* ______ **3559–3562**

The Amphiphilic Properties of Spider Silks Are Important for Spinning

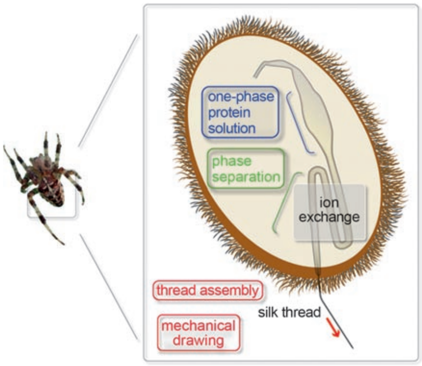

Along came a spider... Spider silk is a fascinating biomaterial owing to its strength, extensibility, and toughness per unit weight which is unrivaled by man-made fibers. The spinning of spider silk corresponds to a transition from a liquid phase to a solid thread. The underlying mechanism of this transition has been investigated using a recombinantly produced spider silk protein.

How nucleophilic are isocyanides? The kinetics of the reactions of alkyl and aryl isocyanides with benzhydrylium ions indicate that isocyanides are 10 orders of magnitude less reactive than the cyanide ion and their nucleophilic reactivity is comparable to that of allylsilanes and silyl enol ethers (see the diagram for a comparison of the nucleophilicity *N* of various isocyanides; Ts = toluene-4-sulfonyl).

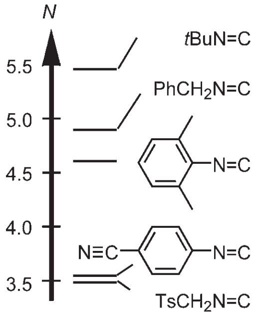

Nucleophilicity

V. V. Tumanov, A. A. Tishkov,
H. Mayr* ——— **3563 – 3566**

Nucleophilicity Parameters for Alkyl and Aryl Isocyanides

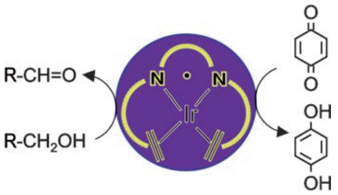

A little goes a long way: An iridium–nitrogen-radical complex is a highly active and selective catalyst for the dehydrogenation (oxidation) of primary alcohols to aldehydes in the presence of the oxidant benzoquinone (see simplified scheme). With only 0.01 mol% of the complex, turnover frequencies of up to 150 000 s^{-1} are reached.

Catalytic Oxidation

M. Königsmann, N. Donati, D. Stein,
H. Schönberg, J. Harmer, A. Sreekanth,
H. Grützmacher* ——— **3567 – 3570**

Metalloenzyme-Inspired Catalysis: Selective Oxidation of Primary Alcohols with an Iridium–Aminyl-Radical Complex

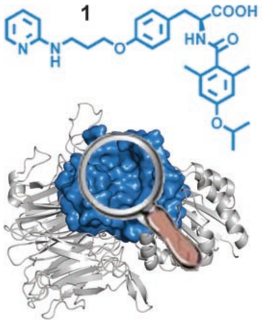

Try and fit in: A strategy for the rational design of α5β1 ligands for the purpose of lead generation and biochemical studies on integrin selectivity is based α5β1 homology modeling. Ligand **1** can bind α5β1 with activities in the subnanomolar range and high selectivity. Minor changes can result in a ligand with a high selectivity for the related αvβ3 receptor.

Integrin Ligands

D. Heckmann, A. Meyer, L. Marinelli,
G. Zahn, R. Stragies,
H. Kessler* ——— **3571 – 3574**

Probing Integrin Selectivity: Rational Design of Highly Active and Selective Ligands for the α5β1 and αvβ3 Integrin Receptor

Two related inhibitors were flexibly docked into different conformers of aldose reductase. Although the overall binding topologies were roughly matched, significant deviations are observed in the subsequently determined crystal structures. Flexible redocking into the crystallographically observed protein conformers achieves, however, perfect binding-position predictions.

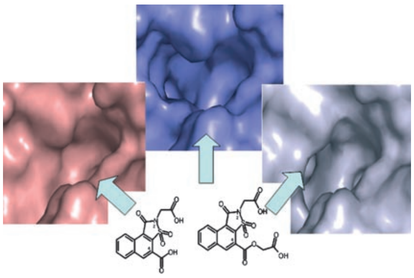

Docking Studies

M. Zentgraf, H. Steuber, C. Koch,
C. La Motta, S. Sartini, C. A. Sotriffer,
G. Klebe* ——— **3575 – 3578**

How Reliable Are Current Docking Approaches for Structure-Based Drug Design? Lessons from Aldose Reductase

Metalloid Clusters

Big Al: Nanometer-separated, perfectly arranged p^1 spin systems are found in crystals of molecular $[Al(Al_3R_3)_2]$ radicals ($R = N(SiMe_2Ph)_2$; see spin-density diagram of the model compound $[Al(AlNH_2)_6]$). $[Al(Al_3R_3)_2]$ is surprisingly stable in the solid state. The unique topology of the seven metal atoms in the $[Al(Al_3R_3)]$ molecules is discussed: Do these atoms represent a section of the bulk structure of Al and can thus be described as the simplest metalloid cluster?

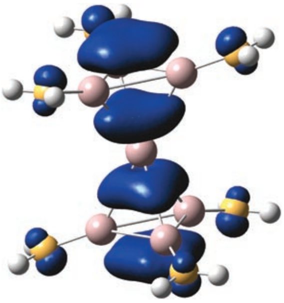

Supporting information is available on the WWW (see article for access details).

A video clip is available as Supporting Information on the WWW (see article for access details).

Service